Supporting Information

Copper-Peptide Complex Structure and Reactivity when Found in Conserved His-X_{aa}-His Sequences

Ga Young Park, [†] Jung Yoon Lee, [†] Richard A. Himes, [†] Gnana S. Thomas,[‡] Ninian J. Blackburn[‡] and Kenneth D. Karlin*,[†]

[†]Department of Chemistry, The Johns Hopkins University, Baltimore, MD 21218, USA.
[‡]Department of Biochemistry and Molecular Biology, OGI School of Science and Engineering at OHSU, Beaverton, Oregon 97006, United States

Contents:

1. Materials and Methods.

General. All materials used were of commercially available reagent quality (Sigma-Aldrich, general reagents; Advanced ChemTech, amino acids; Novabiochem, peptide coupling reagents; Cambridge Isotopes and Sigma-Aldrich, deuterated solvents for NMR spectroscopy) unless otherwise stated. Methanol, methylene chloride and diethyl ether were purified and dried by passing through a double activated alumina column solvent purification system (Innovative Technologies, Inc.). Acetone was distilled from drierite (anhydrous $CaSO_4$) under Ar. Dimethylformamide (DMF, HPLC grade) was used from freshly opened bottles without further purification. Tetrabutylammonium hexafluorophosphate ($TBAPF_6$) was recrystallized twice from 1:1 ethanol-water and dried overnight under vacuum. Carbon monoxide (CO) gas was obtained from Airgas and passed through an oxygen and moisture scrubbing column. $[Cu^{I}(CH_3CN)_4](ClO)_4$ was prepared by the literature procedure.[1] Tripeptide ligands were stored in freezers (-32 °C) in vials wrapped with teflon tape prior to use. Preparation and handling of air-sensitive materials were carried out under an argon atmosphere by using standard Schlenk techniques, within a MBraun Labmaster 130 inertatmosphere drybox filled with prepurified N_2 (Airgas). Deoxygenation of solvents and solutions was achieved by bubbling with Ar for ~30 mins. Solid samples were stored and transferred in the drybox. Samples for UV-vis, IR and NMR spectroscopy were also prepared in the drybox. Samples for conductivity were prepared in the drybox and transferred to Schlenk flask under an inert atmosphere via Schlenk line and performed measurements under high pressure of Ar.

Instrumentation. NMR spectra were measured on Bruker Avance 400 MHz FT-NMR spectrometer, and chemical shifts are reported in ppm (δ) downfield from an internal tetramethylsilane (TMS) reference. Electrospray ionization (ESI) mass spectrometry analyses S4 were performed with a Finnigan LCQ ion trap mass spectrometer with electrospray ionization. Elemental Analyses were performed by Desert Analytics, Tucson, AZ (metal samples). Infrared Spectra were recorded on a Mattson Instruments 4030 Galaxy Series FT-IR spectrometer as solutions in a cell with CaF_2 windows.X-band Electron Paramagnetic Resonance (EPR) spectra were recorded on a Bruker EMX CW-EPR spectrometer controlled with a Bruker ER 041 XG microwave bridge operating at X-band (~ 9 GHz). The low-temperature experiments were carried out via either a continuous-flow He(*l*) cryostat and ITC503 temperature controller made by Oxford Instruments, Inc., or N_2(*l*) finger dewar. All the GC experiments were carried out and recorded using a Hewlett-Packard 5890 Series II Gas Chromatograph. Low Temperature UV-vis Spectra were obtained with a Cary 50 Bio spectrophotometer equipped with a fiber optic coupler (Varian) and a fiber optic dip probe (Hellma: 661.302-QX-UV-2mm-for-low-temperature), and the one equipped with a Unisoku USP-203A cryostat using a 1 cm or 2 mm modified Schlenk cuvette. For the low temperature measurements with a Cary 50 Bio spectrophotometer, a acetone/dry-ice bath (–

80 °C) was used and the steady temperature was monitored with the type T thermocouple thermometer (Model 650, Omega engineering, CT). Air sensitive solutions were prepared in a glove box (N_2 filled, MBraun) and carried out in custom made Schlenk tubes designed for the dip probe (Chemglass: JHU-0407-271MS).

2. Syntheses of Ligands and their Copper(I)/Copper(II) Complexes.

Ligand synthesis.

Compound A (Scheme S1). The Bom group attaches exclusively to N_δ of the histidyl imidazole group. Boc-His(Bom)-OH (1.00 g, 2.7 mmol) was dissolved in DMF (20 ml) and 1 equiv of 2-(1*H*-benzotriazol-1-yl)-1,1,3,3-tetramethyluronium hexafluorophosphate (HBTU), 1 equiv of 1-hydroxybenzotriazole (HOBt), and 2 equiv of diisopropylethylamine (DIPEA) were added under $Ar_{(g)}$. After 10 min, benzyl amine (0.24 g, 2.2 mmol) was added and the reaction stirred under $Ar_{(g)}$ at room temperature. After 16 hrs, the reaction mixture was evaporated under reduced pressure, dissolved in CH_2Cl_2 (40 ml), washed with saturated $NaHCO_{3(aq)}$ three times, saturated $NaCl_{(aq)}$ once, dried ($MgSO_4$) and finally evaporated under reduced pressure. A white solid product was dissolved in 20 ml of 50% trifluoroacetic acid (TFA)-CH_2Cl_2 and stirred at room temperature. After 4 hrs, the mixture was made basic condition (pH 8) with saturated $NaHCO_{3(aq)}$. The organic phase was washed with saturated $NaCl_{(aq)}$ and dried with $MgSO_4$ and evaporated under reduced pressure. The residue was purified by silica gel column chromatography (eluant: CH_2Cl_2:MeOH = 10:1, R_f = 0.5) to give a white solid product (0.51 g, 64%). ^{1}H-NMR ($CDCl_3$) δ 7.65 (s, 1H), 7.49 (d, J = 10 Hz, 1H), 7.24 (m, 10H), 6.91 (d, J = 9.2 Hz, 1H), 5.27 (td, 2H, J = 10.2, 45.2 Hz), 4.47 (m, 4H), 3.65 (m, 1H), 3.27 (m, 1H), 2.88 (m, 1H), 1.52 (s, 1H); ^{13}C-NMR ($CDCl_3$) δ 173.484, 138.484, 138.181, 136.065, 128.593, 128.214, 128.022, 127.806, 127.611, 127.335, 73.158, 69.960, 54.285, 43.103, 29.256; ESI-MS M+H$^+$ $C_{21}H_{25}N_4O_2$ exp m/z: 365.24 (100%), 366.24 (24.8%), 357.24 (4.5%), calc m/z: 365.20 (100.0%), 366.20 (24.6%), 367.20 (3.2%).

Compound B (Scheme S1). Compound **A** (1.6 g, 4.4 mmol) was dissolved in DMF (30 ml) and 1.2 equiv of HBTU, 1.2 equiv of HOBt, 2 equiv of DIPEA, and Boc-Gly-OH (0.925 g, 5.3 mmol) were added and the reaction stirred under $Ar_{(g)}$ at room temperature. After 16 hrs, the reaction mixture was evaporated under reduced pressure, dissolved in CH_2Cl_2 (40 ml), washed with saturated $NaHCO_{3(aq)}$ three times, saturated $NaCl_{(aq)}$ once, dried ($MgSO_4$) and finally evaporated under reduced pressure. A yellow solid product was dissolved in 20 ml of 50% trifluoroacetic acid (TFA)-CH_2Cl_2 and stirred at room temperature. After 4 hrs, the mixture was made basic condition (pH 9) with saturated $NaOH_{(aq)}$. The organic phase was washed with saturated $NaCl_{(aq)}$ and dried with $MgSO_4$ and evaporated under reduced pressure. The residue was purified by silica gel column chromatography (eluant: CH_2Cl_2:MeOH = 10:1, R_f = 0.37) to give a yellowish white solid product (1.4 g, 75%). ^{1}H-NMR ($CDCl_3$) δ 8.20 (s, 1H), 7.42 (s,

1H), 7.26 (m, 10H), 7.08 (s, 1H), 7.07 (s, 1H), 6.86 (s, 1H), 5.19 (br s, 2H), 4.80 (br s, 1H), 4.29 (m, 4H), 3.30 (br s, 2H), 3.09 (m, 4H), 1.31 (s, 1H) 1.52 (s, 1H); ESI-MS $M+H^+$ $C_{23}H_{28}N_5O_3$ exp m/z: 422.11 (100%), 423.11 (28.0%), 424.11 (4.5%), calc m/z: 422.22 (100.0%), 423.22 (26.8%), 424.23 (4.2%).

Ligand ε-HGH (Scheme S1). Compound **B** (0.37 g, 0.88 mmol) was dissolved in DMF (20 ml) and 1.2 equiv of HBTU, 1.2 equiv of HOBt, 2 equiv of DIPEA, and Boc-His(Bom)-OH (0.39 g, 1.05 mmol) were added and the reaction stirred under $Ar_{(g)}$ at room temperature. After 16 hrs, the reaction mixture was evaporated under reduced pressure, dissolved in CH_2Cl_2 (40 ml), washed with saturated $NaHCO_{3(aq)}$ three times, saturated $NaCl_{(aq)}$ once, dried ($MgSO_4$) and finally evaporated under reduced pressure. The residue was purified by silica gel column chromatography (eluant: CH_2Cl_2:MeOH = 10:1, R_f = 0.5) to give a white solid product (0.48 g, 70%). ^{1}H-NMR ($CDCl_3$) δ 7.48 (d, J = 5.1 Hz, 1H), 7.30 (m, 15H), 6.84 (d, J = 6.9 Hz, 2H), 5.62 (d, J = 6.0 Hz, 1H), 5.24 (s, 4H), 4.76 (q, J = 6.9 Hz, 1H), 4.46 (s, 2H), 4.35 (m, 4H), 3.75 (d, J = 4.8 Hz, 1H), 3.11 (m, 4H), 2.08 (s, 1H), 1.33 (s, 9H); ESI-MS $M+H^+$ $C_{42}H_{51}N_8O_7$ exp m/z: 779.40 (100%), 780.40 (45.3%), 781.40 (12.5%), 782.40 (2.8%) calc m/z: 779.39 (100.0%), 780.39 (49.2%), 781.39 (12.9%), 782.40 (2.2%).

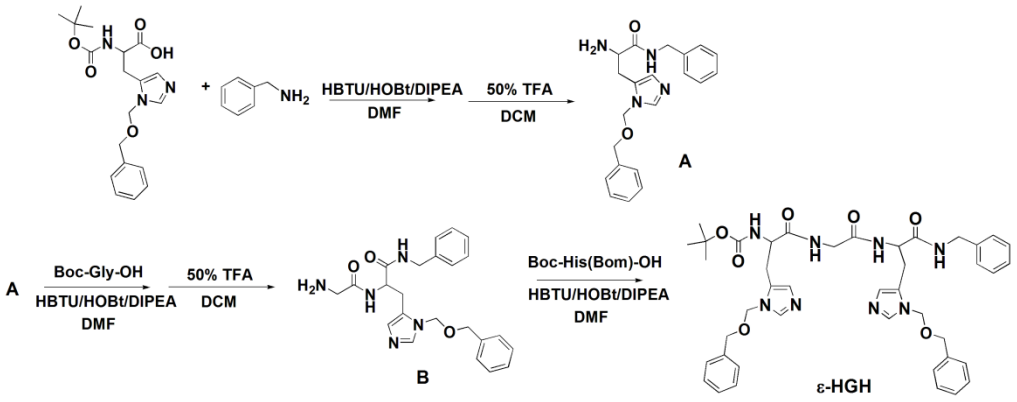

Scheme S1. Synthetic route to the ligand ε-HGH.

Compound C (Scheme S2). Fmoc-His(Trt)-OH (3.41 g, 5.5 mmol) was dissolved in DMF (20 ml) and 1 equiv of HBTU, 1 equiv of HOBt, and 2 equiv of DIPEA were added under $Ar_{(g)}$. After 10 min, benzyl amine (0.5 mL, 5.0 mmol) was added and the reaction stirred under $Ar_{(g)}$ at room temperature. After 16 h, the reaction mixture was evaporated under reduced pressure, dissolved in ethyl acetate (40 ml), washed with saturated $NaHCO_{3(aq)}$ three times, saturated $NaCl_{(aq)}$ once, dried ($MgSO_4$) and finally evaporated under reduced pressure. The compound was dissolved in 20 ml of 20% Piperidine-DMF and stirred at room temperature. After 16 h, solvent was evaporated under reduced pressure and the product was dissolved in ethyl acetate (30 ml) and washed with saturated $NaHCO_{3(aq)}$ three times, saturated

$NaCl_{(aq)}$ once, then dried ($MgSO_4$) and evaporated under reduced pressure. The residue was purified by silica gel column chromatography (eluant: ethyl acetate) to give a yellowish white solid product (1.90 g, 80%). R_f = 0.15 [ethyl acetate]; ^{1}H-NMR ($CDCl_3$) δ 7.87 (br s, 1H), 7.35-7.28 (m, 15H), 7.26-7.11 (m, 6H), 6.65 (s, 1H), 4.40 (dq, 2H, J = 6,15 Hz), 3.69 (m, 1H), 3.08 (dd, 1H, J = 4, 14.5 Hz), 2.79 (dd, 1H, J = 8, 14.5 Hz), 2.18 (br s, 1H); ESI-MS M+H$^+$ $C_{32}H_{31}N_4O$ exp m/z: 487.13 (100%), 488.13 (34.8%), 489.13 (6.5%), calc m/z: 487.25 (100.0%), 488.25 (36.1%), 489.26 (5.9%).

Compound D (Scheme S2). Compound **C** (5.5 g, 11 mmol) was dissolved in 30 ml of DMF and 12 mmol of Fmoc-Gly-OH, 11 mmol of HBTU, 11 mmol of HOBt, and 20 mmol of DIPEA were added. The mixture was stirred under $Ar_{(g)}$ at room temperature. After 16 h, the reaction mixture was evaporated under reduced pressure and the mixture was dissolved in 40 ml of ethyl acetate. The organic phase was washed with saturated $NaHCO_{3(aq)}$ 3 times, saturated $NaCl_{(aq)}$ once, then dried with $MgSO_4$ and evaporated under reduced pressure. The residue was dissolved in 20 ml of 20% Piperidine-DMF and stirred at room temperature. After 16 h, solvent was evaporated under reduced pressure and the product was dissolved in ethyl acetate (30 ml) and washed with saturated $NaHCO_3$ three times, saturated NaCl once, then dried ($MgSO_4$) and evaporated under reduced pressure. Purification by silica gel column chromatography (eluant: ethyl acetate:MeOH = 10:1, R_f = 0.4) gave a yellow solid product (5.0 g, 84%). ^{1}H-NMR ($CDCl_3$) δ 8.25 (s, 1H), 7.40 (s, 1H), 7.31 (m, 20H), 7.11 (s, 1H), 7.08 (s, 1H), 6.86 (s, 1H), 4.42 (dq, 2H, J = 6.2, 16 Hz), 3.71 (m, 1H), 3.12 (dd, 1H, J = 4.2, 14 Hz), 2.79 (m, 3H), 2.18 (br s, 1H); ESI-MS M+H$^+$ $C_{34}H_{34}N_5O_2$ exp m/z: 544.24 (100%), 545.24 (38.0%), 546.24 (6.8%), calc m/z: 544.27 (100.0%), 545.27 (38.6%), 546.28 (7.1%).

Ligand δ-HGH (Scheme S2). Compound **D** (5.0 g, 9.2 mmol) is dissolved in 30 ml of DMF and 11 mmol of Fmoc-His(Trt)-OH, 11 mmol of HBTU, 11 mmol of HOBt, and 20 mmol of DIPEA were added. The mixture was stirred under $Ar_{(g)}$ at room temperature. After 16 h, the reaction mixture was evaporated under reduced pressure and the mixture was dissolved in 40 ml of ethyl acetate. The organic phase was washed with saturated $NaHCO_{3(aq)}$ 3 times, saturated $NaCl_{(aq)}$ once, then dried with $MgSO_4$ and evaporated under reduced pressure. Purification by silica gel column chromatography (eluant: ethyl acetate R_f = 0.4) gave a white solid product (6.42 g, 61%). ^{1}H-NMR (DMSO-d_6) δ 8.43 (s, 1H), 8.32 (s, 1H), 8.25 (s, 1H), 7.88 (d, J = 7.2 Hz, 2H), 7.64 (d, J = 7.2 Hz, 2H), 7.55 (d, J = 8.0 Hz, 1H), 7.29 (m, 34H), 7.03 (m, 14H), 6.72 (s, 1H), 6.62 (s, 1H), 4.55 (q, 1H, J = 5.2 Hz), 4.30 (m, 1H), 4.23 (m, 2H), 4.16 (m, 2H), 4.12 (m, 1H), 3.73 (q, 1H, J = 11.2 Hz), 3.60 (q, 1H, J = 11.6 Hz), 2.92 (m, 2H), 2.74 (m, 2H); ESI-MS M+H$^+$ $C_{74}H_{65}N_8O_5$ exp m/z: 1145.36 (100.0%), 1146.35 (87.0%), 1147.39 (26.0%), 1148.32 (10.0%), 1149.28 (4.1%), calc m/z: 1145.51 (100.0%), 1146.51 (84.0%), 1147.51 (35.0%), 1148.52 (10.3%), 1149.52 (2.0%).

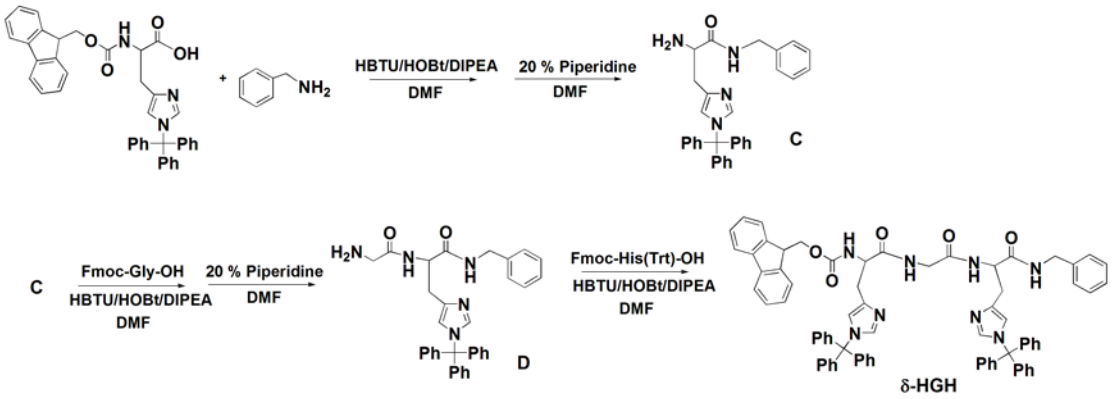

Scheme S2. Synthetic route to the ligand δ-HGH.

Synthesis of Copper(I) Complexes

Caution! *While we have had no problems with this compound, perchlorate salts are potentially explosive and should be handled with great care.*

[{Cu^{I}(δ-HGH)}$_2$](ClO$_4$)$_2$ (1). [Cu^{I}(CH$_3$CN)$_4$]ClO$_4$ (0.14 g, 0.4 mmol) and δ-HGH (0.5 g, 0.4 mmol) are dissolved in CH_2Cl_2 (20 ml) under $Ar_{(g)}$. This mixture was stirred under argon for 30 min then deoxygenated diethylether (100 ml) was added to precipitate. The solid was decanted and washed 2 times with 50 ml of diethylether under Argon. This is redissolved in CH_2Cl_2 and added dropwise to vigorously stirred diethyl ether to give a flocculent white solid isolated by vacuum filtration and dried *en vacuo* (Yield: 0.42 g, 93%). ^{1}H-NMR (DMSO-d$_6$): δ 8.64(br s, 1H), 7.94 (s, 2H), 7.60 (br s, 3H), 7.26 (br m, 35H), 4.73 (s, 1H), 4.16 (br m, 5H), 3.80 (s, 1H), 3.53 (s, 1H), 3.02 (br m, 3H). ESI-MS [Cu(δ-HGH)]$^+$ $C_{74}H_{64}CuN_8O_5$ exp m/z: 1207.70 (100.0%), 1208.68 (76.8%), 1209.59 (74.4%), 1210.56 (36.8%), 1211.54 (13.9%), 1212.54 (3.5%), calc m/z: 1207.43 (100.0%), 1208.43 (83.2%), 1209.43 (80.3%), 1210.43 (47.6%), 1211.43 (18.1%), 1212.44 (4.3%). Anal. Calcd. for $C_{74}H_{64}Cl_1CuN_8O_9\cdot(CH_2Cl_2)_3$: C, 59.16; H, 4.51; N, 7.17; Found: C, 59.43; H, 4.31; N, 7.14.

[Cu^{I}(ε-HGH)]ClO$_4$ (2). [Cu^{I}(CH$_3$CN)$_4$]ClO$_4$ (0.18 g, 0.53 mmol) and ε-HGH (0.5 g, 0.64 mmol) are dissolved in CH_2Cl_2 (20 ml) under $Ar_{(g)}$. This mixture was stirred under argon for 30 min then deoxygenated diethylether (100 ml) was added to precipitate. The solid was decanted and washed 2 times with 50 ml of diethylether under Argon. This is redissolved in CH_2Cl_2 and added dropwise to vigorously stirred diethyl ether to give a flocculent white solid isolated by vacuum filtration and dried *en vacuo* (Yield: 0.50 g, 83%). ^{1}H-NMR (DMSO-d$_6$): δ 8.63 (t, J = 6.0 Hz, 1H), 8.45 (d, J = 8.8 Hz, 1H), 8.17 (s, 2H), 7.25 (m, 17H), 6.77 (s, 2H), 6.65 (s, 1H), 5.54 (br m, 4H), 4.80 (t, J = 10.2 Hz, 1H), 4.50 (br m, 4H), 4.32 (d, J = 5.6 Hz, 2H), 4.01 (q, J = 6.0 Hz, 1H), 3.63 (d, J = 16.8 Hz, 1H), 3.26 (d, J = 15.2 Hz, 1H), 3.00 (br m, 3H), 1.35 (s, 9H). ESI-MS [Cu(ε-HGH)]$^+$ $C_{42}H_{50}CuN_8O_7$ exp m/z: 841.30 (100.0%), 842.30 (43.5%), 843.30 (48.9%), 844.30 (19.8%), 845.30 (6.2%), 846.30 (1.3%), calc m/z: 841.31 (100.0%),

842.31 (48.6%), 843.31 (57.9%), 844.31 (24.5%), 845.31 (5.8%), 846.32 (1.0%). Anal. Calcd. for $C_{42}H_{50}ClCuN_8O_{11}\cdot H_2O$: C, 52.55; H, 5.46; N, 11.67; Found: C, 52.82; H, 5.32; N, 11.63.

Synthesis of Copper(II) Complexes

$[Cu^{II}(\varepsilon\text{-HGH})(H_2O)](ClO_4)_2$. $Cu^{II}(ClO_4)_2\cdot 6H_2O$ (0.18 g, 0.5 mmol) and ε-HGH (0.3 g, 0.50 mmol) are dissolved in MeOH (20 ml) under Air. This mixture was stirred under argon for 30 min then diethylether (100 ml) was added to precipitate. The solid was decanted and washed 2 times with 50 ml of diethylether. This is redissolved in MeOH and added dropwise to vigorously stirred diethyl ether to give a blue solid isolated by vacuum filtration and dried *en vacuo* (Yield: 0.23 g, 44%). Anal. Calcd. for $C_{42}H_{50}Cl_2CuN_8O_{15}\cdot H_2O$: C, 47.62; H, 4.95; N, 10.58; Found: C, 47.54; H, 4.81; N, 10.38. UV-vis (acetone; λ_{max}, nm; ε, $M^{-1}cm^{-1}$): 649; 40 (see Figure S6). X-band spectrometer (ν = 9.468 GHz) in acetone at 4 K; g = 2.064, g_{ll} = 2.31, A_{ll} = 162 gauss.

3. IR Spectra for CO-adducts of the Copper(I) Complexes.

IR samples were prepared as millimolar solutions in ~ 2 mL of degassed acetone and DMF (for **1** and **2**) in Schlenk flasks sealed with rubber septa. These solutions were bubbled for ~ 30 s with CO, then a small portion of the solution was transferred to an IR cell via syringe. Spectra recorded were the average of 16 scans, $2cm^{-1}$ resolution.

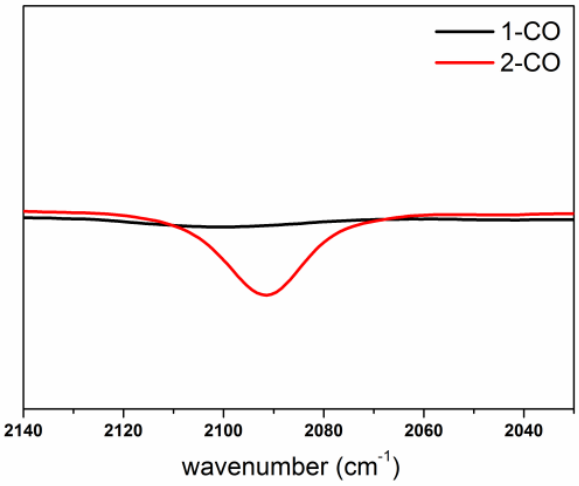

Figure S1. Solution IR spectra of 10 mM **1**-CO (black) and 10 mM **2**-CO (red) in acetone.

4. Electrochemistry.

Cyclic voltammetry was carried out using a Bioanalytical Systems BAS-100B Electrochemistry Analyzer. The cell consisted of a three-necked round bottom flask. The electrodes were inserted into the cell through hole-punched rubber septa, allowing for the entire system to be kept under an inert (Ar-N_2)

atomosphere. A glassy carbon electrode, polished with diamond solution prior to each measurement, was used as the working electrode. The reference electrode was $Ag/AgNO_3$ in a 0.1M $TBAPF_6$ in acetonitrile solution. A platinum wire was used as the counter electrode. The measurements were performed at room temperature under an Ar atmosphere in DMF solution containing 0.1 M $TBAPF_6$ and 10^{-3} M copper complex.

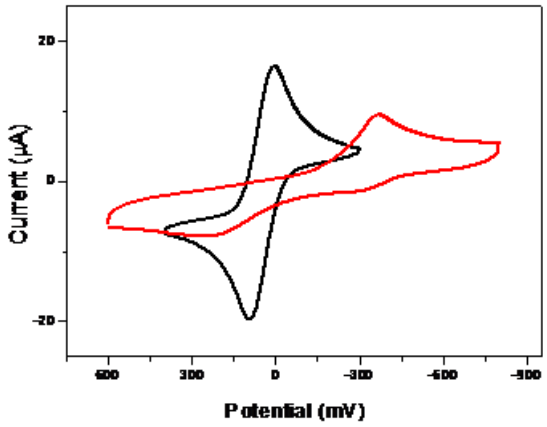

Figure S2. Cyclic voltammagrams of the 2-coordinate Cu^I complex $[\{Cu^I(\delta\text{-HGH})\}_2]^{2+}$ (**1**) (DMF, 100mM $TBAPF_6$, 1mM Cu complex). Comparison of **1** (red) with ferrocene (black), scan rate = 100mV/s.

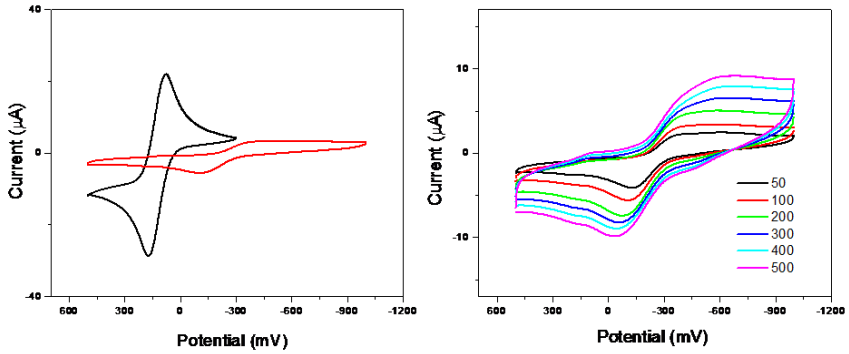

Figure S3. Cyclic voltammagrams of two-coordinate Cu^I complex $[Cu^I(\varepsilon\text{-HGH})]^+$ (**2**) (DMF, 100mM $TBAPF_6$, 1mM Cu complex). Left: Comparison of **2** (red) with ferrocene (black), scan rate = 100mV/s. Right: Complex **2**, varying scan rates (from 50 mV/s to 500 mV/s).

5. Conductivity Experiments and Onsager Plots.

Conductivity measurements were carried out in DMF with an Accumet AR-20 Conductivity meter at 25 °C, using an Accumet conductivity cell (cell constant K=1.0 cm^{-1}). The 1:1 electrolyte $[(TMPA)Cu^{II}Cl]ClO_4$ [2] (with Onsager plot slopes of 864 in acetone[3] and 270.5 in DMF) and the 2:1 electrolyte $[(TMPA)Cu^{II}(H_2O)](ClO_4)_2$ [4] (with Onsager plot slopes of 1550 in acetone and 578.4 in DMF) were used as standards. The data obtained from the measurements were used to calculate Λ_e, the

equivalent conductivity at different concentrations. A plot of Λ_e as a function of the square root of concentration ($c^{1/2}$), followed by extrapolation through a linear least-squares fit resulted in Λ_0, the conductivity at infinite dilution, as the y intercept. Onsager plots were then constructed by plotting the difference, Λ_0-Λ_e, as a function of $c^{1/2}$.

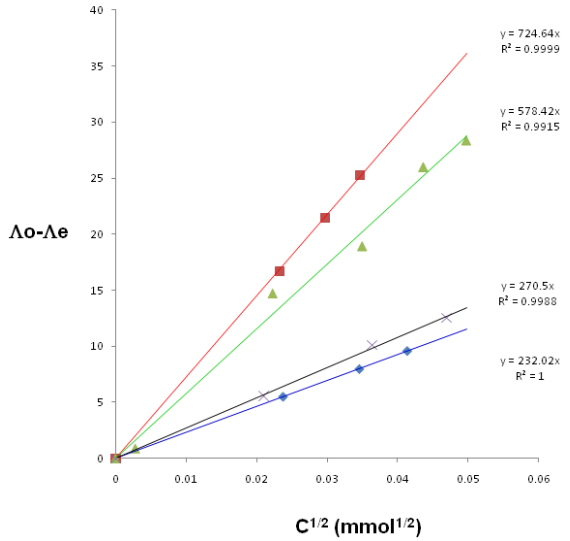

Figure S4. Onsager plots of **1** (red), **2** (blue), the 1:1 electrolyte $[(TMPA)Cu^{II}Cl]ClO_4$ (black) and the 2:1 electrolyte $[(TMPA)Cu^{II}(H_2O)](ClO_4)_2$ (green) in DMF, with linear fits.

6. XAS Data Collection and Analysis.

For Cu K-edge powder spectra, the peptide samples were ground into a fine powder and diluted in boron nitride. The mixture was then packed into an aluminum spacer sample holder, sealed with Mylar tape and then transferred to a liquid He cryostat on the beam line. X-ray absorption spectroscopy was carried out at the Stanford Synchrotron Radiation Light Source with the spear storage ring operating at 3.0 GeV with beam currents between 100 and 80 mA. Cu K-edge (8.9 keV) extended x-ray absorption fine structure (EXAFS) and x-ray absorption near edge structure (XANES) data were collected on beam line 9-3, employing wiggler fields of 2 T. The beam line was configured with a liquid nitrogen cooled Si[220] monochromators to provide monochromatic radiation in the 8.8 - 9.7 keV energy range. Harmonic rejection was achieved by a Rh-coated mirror downstream of the monochromator set to an energy cut-off of 13 KeV. The powder samples were measured in transmission mode at 10 – 16 K using a 30 element Canberra Ge detector. Energy calibration was achieved by reference to the first inflection point of a copper foil (8980.3 eV) placed between the second and third ionization chambers. Data reduction and background subtraction were performed using the program modules of EXAFSPAK.[5] Spectral simulation was carried out using the program EXCURVE 9.2 as described previously.[6-9] This allowed for inclusion of multiple scattering pathways between the metal center and the atoms of imidazole rings of the histidine

residues. Parameters refined in the fits were coordination numbers, distances, and Debye-Waller factors (DW) for metal-ligand interactions. E_f, a small correction to the threshold energy E_0, was also refined but was constrained to take the same value for all shells of scatterers. The amplitude reduction factor was set at 0.90. The goodness of fit was judged by a fitting parameter, F, defined as

$$F^2 = \frac{1}{N}\sum_{i=1}^{N} k^6 (Data_i - Model_i)^2$$

where N is the number of data points.

Table S1. Fits obtained to the EXAFS of the solid samples $[\{Cu^I(\delta\text{-HGH})\}_2]^{2+}$ (**1**) and $[Cu^I(\varepsilon\text{-HGH})]^+$ (**2**) by Curve-Fitting using the program EXCURV 9.2

Cu Complexes	Cu K-edge EXAFS					
	Scatterers	No	Distance (Å)	Debye-Waller (Å)	$-E_0$ (eV)	F
$[\{Cu^I(\delta\text{-HGH})\}_2]^{2+}$ (**1**) Two Imidazole ligands	N (donor)	2	1.876	0.007	2.982	0.50
	C_2	2	2.937	0.010		
	C_3	2	2.823	0.010		
	N_4	2	4.016	0.015		
	C_5	2	4.158	0.015		
$[Cu^I(\varepsilon\text{-HGH})]^+$ (**2**) Two Imidazoles (**ε**-histidine coordination as expected)	N (donor)	2	1.878	0.007	2.174	0.35
	C_2	2	2.895	0.013		
	C_3	2	2.862	0.013		
	N_4	2	4.070	0.017		
	C_5	2	4.107	0.017		

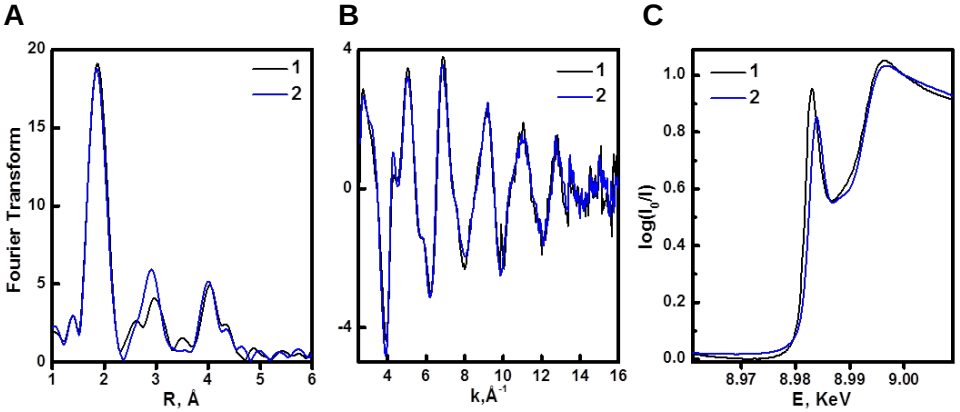

Figure S5. Overlapped EXAFS (**A** and **B**) and XANES (**C**) spectroscopic data for $[\{Cu^I(\delta\text{-HGH})\}_2]^{2+}$ (**1**) (black line) and $[Cu^I(\varepsilon\text{-HGH})]^+$ (**2**); (blue line) for comparison.

7. Computational Details.

All DFT calculations were carried out using the Gaussian 09 package (Revision D.01)[10] and made use of the restricted B3LYP hybrid functional.[11] Geometries were confirmed as minima based on the frequency calculations (NIm = 0). Single point energy calculations were carried out at the B3LYP/6-311++G(2df,2pd) level of theory on the B3LYP/6-311G** optimized structures. Zero-point energy corrections and thermal corrections to the Gibbs free energy [B3LYP/6-311G**] were scaled by 0.9877 according to this reference (New Scale Factors for Harmonic Vibrational Frequencies Using the B3LYP Density Functional Method with the Triple-ζ Basis Set 6-311+G(d,p))[12] and applied to the single point energies.

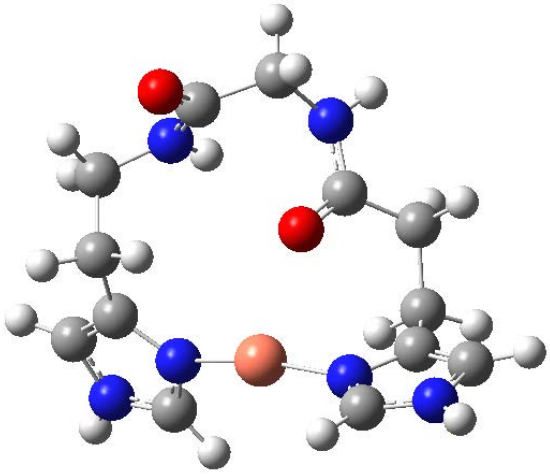

Figure S6. DFT optimized geometry (RB3LYP/6-311G**) of mononuclear species, $[Cu^{I}(\delta\text{-HGH})]^{+}$; $\angle$ δN-Cu- δN = 168.3°, Cu-N : 1.892, 1.879 Å, possible long interaction between Cu and a backbone carbonyl O : ~2.5 Å.

Table S2. Final coordinates of optimized $[Cu^{I}(\delta\text{-HGH})]^{+}$ model (RB3LYP/6-311G**).

C	-4.34781600	0.13063000	-0.08719200
C	-3.22239000	-1.01693200	-1.60510300
H	-1.71523400	-0.52426000	1.94730700
H	1.53995800	4.37667600	0.63717900
C	-3.09172400	-0.13219100	0.38623700
H	-2.99812900	-1.53458800	-2.52277400
O	-0.46808000	1.20041100	-0.15526000
H	2.83177500	-4.13474400	1.67896300
C	-2.46599400	0.23217400	1.70174300
H	2.19308300	1.46082500	1.09782200
N	-2.40342400	-0.85597600	-0.57941000
H	-3.22898800	0.16784700	2.48184800

C	0.99364000	3.56548000	0.15111300
H	4.34099400	-2.52286700	0.41287000
C	-0.66486900	1.88073700	0.84395000
H	0.39165000	3.99562500	-0.65205700
N	2.49249900	-3.36591800	1.12052300
H	4.20020600	0.35747300	0.27233800
N	2.58415500	1.66996200	0.19296600
C	3.26594900	-2.46783200	0.41982700
N	0.14605300	2.93057900	1.16376900
C	-1.83073100	1.63332500	1.79394900
C	2.01595200	2.66369300	-0.54845300
H	0.37747000	-3.61007300	1.33830900
C	1.19910400	-3.05822000	0.91368900
C	3.46863800	0.71559200	-0.45554400
H	-1.51308700	1.81334100	2.82614600
H	-0.11574500	3.49850800	1.95639800
C	2.39922400	-1.61114800	-0.20828900
H	-2.58796300	2.39424600	1.57130000
H	4.00248000	1.26780700	-1.22787700
O	2.32931300	2.90245100	-1.69821400
N	1.10244600	-1.99784600	0.11633500
C	2.73211800	-0.47301500	-1.12464900
H	3.36852400	-0.85233800	-1.92999100
H	-5.20559100	-0.41496800	-1.96473900
H	-5.18568900	0.64549700	0.35077000
N	-4.40900700	-0.42904200	-1.34588300
Cu	-0.57587000	-1.28073400	-0.33169400
H	1.81900600	-0.10168200	-1.59267100

Table S3. Final coordinates of optimized $[\{Cu^{I}(\delta\text{-HGH})\}_2]^{2+}$ (**1**) model (RB3LYP/6-311G).

Cu	2.74282	6.60719	3.50344
Cu	10.78785	-0.43141	2.65993
C	-0.04044	3.69396	2.7165
C	1.23354	3.94828	3.07236
C	0.23593	5.94147	2.70742
N	-0.82645	4.93605	2.70291
H	-1.44146	5.0093	1.92104
H	-0.42809	2.72624	2.48365
H	0.1068	6.97209	2.43589
N	1.36192	5.42656	3.07881
C	2.22356	2.77841	3.36889
H	2.16676	2.52753	4.4107
H	1.90555	1.95171	2.77049

C	3.70674	3.06159	3.01989
H	3.78627	3.39846	2.01178
H	4.10999	3.81111	3.67671
C	4.47198	1.70612	3.1774
N	5.65517	1.39352	2.34313
H	5.37067	1.24526	1.39882
O	4.04646	0.8479	4.00522
C	6.28993	0.14064	2.81916
H	5.56401	-0.65073	2.76166
H	6.62308	0.24717	3.83312
C	7.49816	-0.21973	1.90268
O	8.38798	-1.00854	2.32688
N	7.59518	0.37167	0.54329
H	7.01862	-0.12999	-0.09899
C	8.97865	0.35231	0.00609
H	9.03586	0.99309	-0.84951
H	9.65296	0.68692	0.7634
C	9.34295	-1.07676	-0.47594
H	10.32668	-1.08545	-0.89564
H	8.62792	-1.35643	-1.22009
C	9.28553	-2.09817	0.66914
C	8.71765	-3.32405	0.58707
N	8.98968	-4.05359	1.82875
H	8.14766	-3.69275	-0.24494
C	9.47852	-2.95623	2.71799
H	8.19659	-4.53918	2.18994
H	9.55591	-3.02224	3.7776
N	9.8068	-1.91339	2.02728
C	5.09379	9.88896	4.31625
C	5.08045	8.61637	3.88385
C	2.96278	9.13757	4.45037
N	3.72578	10.38348	4.47551
H	3.58955	10.91321	5.30912
H	5.97436	10.45925	4.51856
H	1.95447	9.02775	4.8026
N	3.6639	8.16814	3.95708
C	6.41563	7.94988	3.47199
H	6.5579	8.06319	2.41107
H	7.19604	8.45532	4.0061
C	6.51413	6.45661	3.82481
H	6.29714	6.30261	4.8617
H	5.82858	5.87194	3.23878
C	7.97968	6.05224	3.56123
N	8.58638	4.96779	4.36138

H	8.74945	5.28275	5.29493
O	8.64576	6.6713	2.68356
C	9.88164	4.57501	3.78441
H	10.56894	5.40341	3.87283
H	9.76488	4.32587	2.75047
C	10.4294	3.35049	4.55206
O	11.22871	2.55846	3.9809
N	10.00819	3.08251	5.94284
H	10.68265	3.44276	6.58822
C	9.88379	1.62788	6.08833
H	9.48613	1.37637	7.06135
H	9.2192	1.27248	5.33159
C	11.27477	0.97483	5.90757
H	11.15417	-0.07963	5.84935
H	11.90677	1.23269	6.73857
C	11.9423	1.5155	4.63867
C	12.77953	2.5744	4.63276
N	13.03782	2.95317	3.24642
H	13.19732	3.06881	5.49782
C	12.58589	1.74508	2.51823
H	12.49397	3.74823	2.99428
H	12.85785	1.5071	1.51593
N	11.8212	1.00848	3.26671

Table S4. Final coordinates of optimized $[Cu^{I}(\varepsilon\text{-HGH})]^{+}$ (**2**) model (RB3LYP/6-311G**).

H	-0.12640000	2.64100000	1.63200000
O	-1.92890000	1.11130000	1.68690000
H	4.47570000	1.57150000	0.89080000
H	-2.61870000	-3.37200000	1.05730000
H	2.23090000	3.23570000	0.86180000
H	-4.39380000	1.37880000	1.16340000
C	-2.37150000	1.84460000	0.81790000
C	-2.57460000	-2.50280000	0.42290000
H	-4.45210000	-1.64470000	0.80190000
H	1.65970000	-0.10500000	-1.16230000
C	-0.25550000	3.06750000	0.63430000
C	4.14270000	1.21260000	-0.09020000
N	2.06940000	2.65000000	0.05520000
C	2.33280000	-0.60890000	-0.48950000
N	-3.57520000	-1.60380000	0.30450000
H	5.04530000	1.12470000	-0.70650000
C	3.48140000	-0.12120000	0.05850000
H	-0.06110000	4.14270000	0.69700000

N	-1.62650000	2.84100000	0.24960000
Cu	0.28310000	-2.33970000	-0.18550000
N	2.08200000	-1.88560000	-0.00560000
C	-3.80150000	1.69500000	0.30300000
N	-1.56080000	-2.15550000	-0.35540000
C	0.77460000	2.42250000	-0.31270000
N	3.94350000	-1.14090000	0.87570000
C	3.07740000	-2.17930000	0.81430000
H	4.79560000	-1.12950000	1.41650000
C	3.23260000	2.27320000	-0.74330000
H	-4.20740000	2.64890000	-0.04440000
C	-3.18650000	-0.61460000	-0.58070000
H	3.19950000	-3.09700000	1.36490000
H	3.83270000	3.16590000	-0.93740000
C	-1.94000000	-0.98230000	-0.99130000
H	-2.00400000	3.36290000	-0.52500000
O	0.45030000	1.76900000	-1.29140000
C	-3.93240000	0.65150000	-0.84380000
H	-1.28670000	-0.45020000	-1.66250000
H	2.85830000	1.91990000	-1.70420000
H	-4.99430000	0.45730000	-1.02140000
H	-3.53720000	1.07410000	-1.77010000

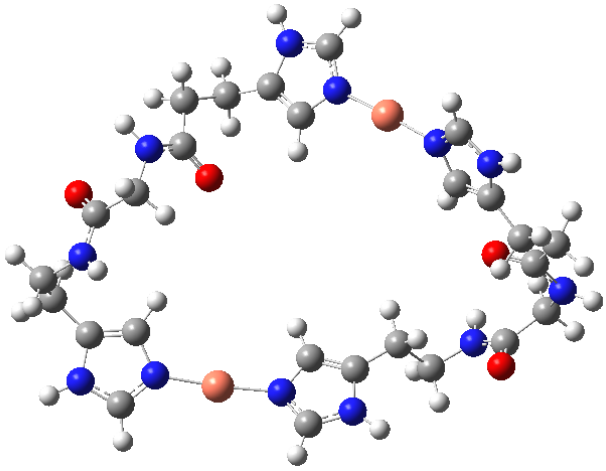

Figure S7. DFT optimized geometry (RB3LYP/6-311G**) of dinuclear species, $[\{Cu^{I}(\varepsilon\text{-HGH})\}_2]^{2+}$; ∠εN-Cu-εN = 173 °.

Table S5. Final coordinates of optimized $[\{Cu^{I}(\varepsilon\text{-HGH})\}_2]^{2+}$ model (RB3LYP/6-311G**).

H	-0.12492400	6.51493500	-2.53623900
H	2.09954100	6.39473100	-1.33244300
N	0.16968500	5.72123100	-1.98600900
C	1.34935500	5.62194200	-1.33859800

H	-1.09437800	-5.73939700	1.44749500
H	-2.01748200	4.97109000	-3.27861900
H	-1.95039000	3.29442200	-2.76509700
C	-0.55000500	4.55240900	-1.80235500
N	1.43057500	4.44434800	-0.73520200
H	4.93282100	4.41217400	2.56603200
C	-1.90215800	4.32322600	-2.40516300
H	-6.12584100	-4.80280600	0.81646200
C	-0.69125200	-5.00413500	0.77139700
H	6.47257500	2.57305900	3.37590400
Cu	-3.19752000	-3.68932500	0.13075500
C	0.25184000	3.77120400	-1.01555900
H	1.36647000	-5.39962400	0.93823100
C	4.97977100	3.41372900	2.16497600
H	-8.08522400	-3.20750900	0.64770800
N	5.81423500	2.45643500	2.61939500
N	-1.38690100	-4.11982000	0.07157500
N	0.62642400	-4.85645200	0.51627400
C	-6.06507400	-3.76563700	0.53227700
N	-7.12930200	-2.93825800	0.46405900
H	-4.01075600	4.59201800	-2.03747600
N	4.24984800	2.93099300	1.16871700
H	0.03892900	2.78816300	-0.63371200
C	-3.08503000	4.55796900	-1.45212500
H	5.64397100	-0.74072100	2.50211400
Cu	2.85797600	3.72908000	0.22427200
N	-4.96554800	-3.10996100	0.18997600
H	6.99664200	0.20924100	3.06870700
C	5.61952100	1.29508600	1.88869900
O	-6.45128200	2.45992700	-0.21289900
H	-3.00263000	5.52341000	-0.94350800
H	-8.62410200	-0.85664700	-0.38035800
C	-0.46704700	-3.38406000	-0.65917900
C	0.79899100	-3.82500600	-0.39158900
C	6.36106500	0.02649600	2.19749900
C	4.64096400	1.61465100	0.98645600
C	-6.70732500	-1.68584300	0.04972700
H	2.75997600	-3.08927600	-0.01397600
C	-3.25151200	3.44429100	-0.41940100
C	-5.35481900	-1.81412100	-0.11345700
H	-4.78283800	4.50272400	0.39499200
H	-0.77111600	-2.58921100	-1.31911600
O	-2.62202800	2.39682500	-0.46613300
C	-7.62047100	-0.51455800	-0.10870900

H	-8.46303500	1.16771600	0.93024500
O	5.07641900	-4.20247900	0.00247600
H	4.23028600	0.97890500	0.22346200
N	-4.16316400	3.72210000	0.55921200
C	2.13183600	-3.35634200	-0.86802900
H	3.04667400	-5.31339300	-1.15665500
C	-5.95179300	2.04713300	0.81833800
H	-4.64861500	-1.06740000	-0.43538500
H	-7.26877400	0.10848400	-0.93213700
C	-7.73426300	0.38326800	1.14587700
C	7.25434500	-0.54181000	1.07513900
H	1.98535500	-2.44552000	-1.45288700
H	7.99405800	-1.20936700	1.52518500
C	2.91116500	-4.38719700	-1.71887400
C	-4.67847600	2.67785000	1.41383600
N	-6.47111900	1.00594300	1.52684300
C	5.20478500	-3.77770600	-1.13125500
H	-4.89838600	3.08233000	2.40633900
C	6.47980900	-1.28579200	-0.00809000
H	7.81553900	0.26455000	0.59110100
O	5.35692500	-0.95447000	-0.37240000
H	2.36796600	-4.62670100	-2.63452300
H	-8.09718600	-0.18682900	2.00310600
H	7.99161900	-2.66505600	-0.17322400
N	7.13205600	-2.33143900	-0.57741000
N	4.22649300	-3.88308700	-2.07506000
H	-3.90091400	1.91962000	1.52040200
H	-6.03496300	0.73270400	2.39321600
C	6.50186100	-3.11346900	-1.62112600
H	7.19603100	-3.89858400	-1.92742400
H	4.33591700	-3.39814700	-2.95178400
H	6.30420800	-2.48113100	-2.49114900

8. Dioxygen Reactivity of $[\{Cu^{I}(\delta\text{-HGH})\}_2](ClO_4)_2$ (1) and $[Cu^{I}(\varepsilon\text{-HGH})]ClO_4$ (2)

Complex **2** (0.015 g, 16 μmol) was dissolved in 7 ml acetone in the drybox and then was brought out and cooled to –80 °C using an acetone/dry-ice bath. The $[Cu^{I}(\varepsilon\text{-HGH})]ClO_4$ (**2**)/O_2 reaction in acetone results in the formation of the metastable complex at –80 °C, which exhibits absorptions at 336 nm (ε = 1110 $M^{-1}cm^{-1}$) and 606 nm (ε = 110 $M^{-1}cm^{-1}$) (Figure S5-A). A frozen solution EPR measurement of this low-temperature meta-stable species indicates it is diamagnetic (i.e., EPR silent). However, small amount (compare to decomposition product) of a typical tetragonal EPR (g = 2.055) is observed (Figure S5-C), and it could be suggested that the bridged structure breaks. Warming this low-temperature meta-stable

species to RT (λ_{ex} = 616 nm (ε = 80 $M^{-1}cm^{-1}$), (Figure S5-A); EPR spectrum in acetone at 77 K: $g_{\|}$ = 2.25, $g_{\perp}$ = 2.035, $A_{\|}$ = 185 (Figure S5-D)).

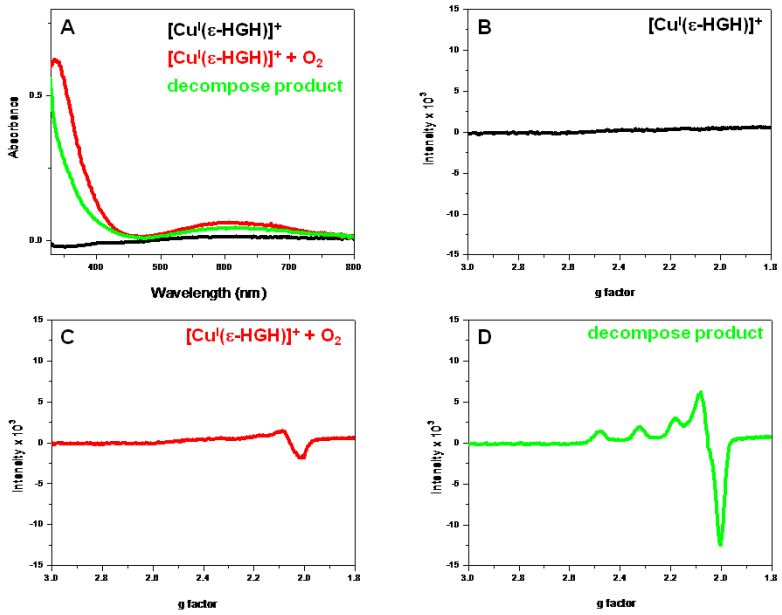

Figure S8. **A.** Absorbance spectra of [Cu^{I}(ε-HGH)]$^{+}$ (**2**) (black) and [Cu^{I}(ε-HGH)]$^{+}$ + O_2 (red; 336 nm (ε = 1110 $M^{-1}cm^{-1}$) and 606 nm (ε = 110 $M^{-1}cm^{-1}$)) and its thermal decompose product (green) in acetone. **B.** EPR spectrum of **2** taken with an X-band spectrometer (ν = 9.186 GHz) in acetone at 77 K; EPR silent. **C.** EPR spectrum of [Cu^{I}(ε-HGH)]$^{+}$ + O_2 taken with an X-band spectrometer (ν = 9.186 GHz) in acetone at 77 K; EPR silent with small amount of g = 2.055. **D.** EPR spectrum of a thermal decompose product taken with an X-band spectrometer (ν = 9.186 GHz) in acetone at 77 K; $g_{\|}$ = 2.25, $g_{\perp}$ = 2.035, $A_{\|}$ = 185.

9. Hydrogen Peroxide Quantification.

Detection of H_2O_2 as a product has been performed with CH_3CN-saturated NaI solution as in a literature.[13] 2.5 mL of a 0.6 mM acetone solution of [Cu^{I}(ε-HGH)]$(ClO)_4$ (**2**) was charged in a 1 cm modified Schlenk cuvette and the cuvette was sealed with a rubber septum in a glove box. Out of the glove box, the solution cooled to –80 °C and dioxygen was gently bubbled through the solution. After the green-colored Cu^{I}/O_2 species was generated, the solution was taken out and warmed to room temperature (RT). 70 μL of the solution was added into 2.0 mL of a CH_3CN-saturated NaI solution at room temperature in the darkness. This mixture was allowed to incubate for one min. The UV-vis spectrum displayed the formation of triiodide (I_3^-) at 362 nm and the yield was calculated by comparing with a standard H_2O_2 solution of known concentrations.

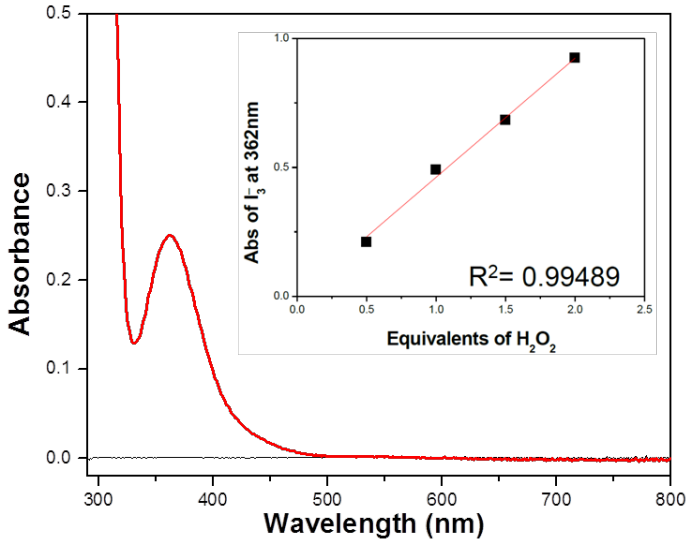

Figure S9. UV-vis spectrum of triodide (I_3^-) at 362 nm produced from **2** + O_2 reaction. Inset : standard of titration with authentic H_2O_2 solutions (stock solution, 0.6 mM).[13]

10. Generation of $[Cu^{II}(\varepsilon\text{-HGH})(OOH)]^+$

From the reaction of $[Cu^{I}(\varepsilon\text{-HGH})]ClO_4$ (2) and H_2O_2. Complex **2** (7.2 mg) was dissolved in 2 ml acetone in the drybox and 500 µL solution was transferred into the 2 mm modified Schlenk cuvette. The 2 mm Schlenk cuvette was sealed with a rubber septum. Then the cuvette was taken out and cooled to –80 ºC for 10 min. Addition of 3/2 equivalent of 50 wt % H_2O_2 (0.116 µL in 50 µL acetone solution) (Aldrich) led to the formation of green complex $[Cu^{II}(\varepsilon\text{-HGH})(OOH)]^+$, λ = 366 nm (ε = 2600 $M^{-1}cm^{-1}$) and 600 nm (ε = 200 $M^{-1}cm^{-1}$) (See Figure 4). The generation of hydroperoxo species took about 2 hrs to fully form. X-band EPR of $[Cu^{II}(\varepsilon\text{-HGH})(OOH)]^+$, in acetone at 77 K: $g_{\|}$ = 2.25, $g_{\perp}$ = 2.05, $A_{\|}$ = 192 G, $A_{\perp}$ = 15 G (See Figure 4).

From the reaction of $[Cu^{II}(\varepsilon\text{-HGH})(H_2O)](ClO_4)_2$ and H_2O_2/Et_3N. $[Cu^{II}(\varepsilon\text{-HGH})(H_2O)](ClO_4)_2$ (3.7 mg) was dissolved in 10 ml acetone and 2.5 mL solution was transferred into 1 cm modified Schlenk cuvette. The Schlenk cuvette was sealed with a rubber septum. Then the cuvette was cooled to –80 ºC for 10 min. Addition of 10 equiv H_2O_2 (50 wt %) (Aldrich) and 2 equiv Et_3N immediately led to the formation of green complex $[(\varepsilon\text{-HGH})Cu^{II}(^-OOH)]^+$, λ = 369 nm (ε = 2800 $M^{-1}cm^{-1}$) and 595 nm (ε = 160 $M^{-1}cm^{-1}$). X-band EPR of $[(\varepsilon\text{-HGH})Cu^{II}(^-OOH)]^+$, in acetone at 77 K: $g_{\|}$ = 2.250, $g_{\perp}$ = 2.048, $A_{\|}$ = 191 G, $A_{\perp}$ = 16 G.

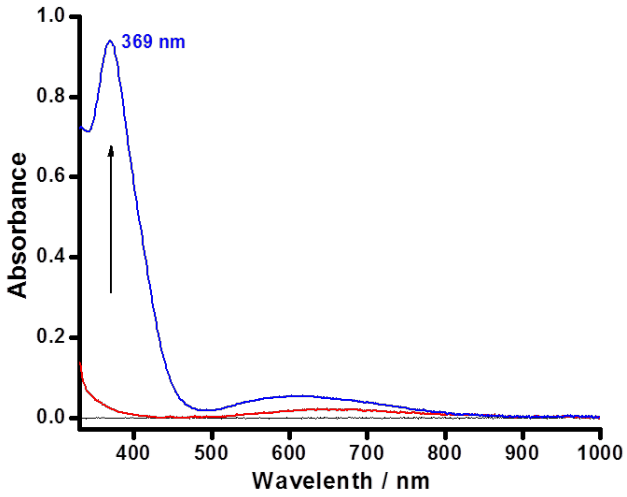

Figure S10. UV-vis spectra of $[Cu^{II}(\varepsilon\text{-HGH})(H_2O)](ClO_4)_2$ in acetone (red) and $[(\varepsilon\text{-HGH})Cu^{II}(^{-}OOH)]^{+}$ from the reaction of $[Cu^{II}(\varepsilon\text{-HGH})(H_2O)](ClO_4)_2 + H_2O_2/Et_3N$ in acetone at –80 °C (blue).

11. References

1. Liang, H. C.; Karlin, K. D.; Dyson, R.; Kaderli, S.; Jung, B.; Zuberbuhler, A. D. *Inorg. Chem.* **2000**, *39*, 5884-94.

2. Wei, N., State University of New York at Albany, 1994.

3. Zhang, C. X.; Kaderli, S.; Costas, M.; Kim, E.; Neuhold, Y. M.; Karlin, K. D.; Zuberbuhler, A. D. *Inorg. Chem.* **2003**, *42*, 1807-24.

4. Jacobson, R. R., State University of New York at Albany, 1989.

5. George, G. N. *EXAFSPAK*; Stanford Synchrotron Radiation Laboratory: Menlo Park, CA, 1990.

6. Binsted, N. G., S. J.; Campbell, J. W. *EXCURVE 9.2* Daresbury Laboratory, Warrington, England, 1998.

7. Gurman, S. J.; Binsted, N.; Ross, I. *Journal of Physics C-Solid State Physics* **1984**, *17*, 143-51.

8. Gurman, S. J.; Binsted, N.; Ross, I. *Journal of Physics C-Solid State Physics* **1986**, *19*, 1845-61.

9. Binsted, N.; Hasnain, S. S. *Journal of Synchrotron Radiation* **1996**, *3*, 185-96.

10. M. J. Frisch, G. W. Trucks, H. B. Schlegel, G. E. Scuseria, M. A. Robb, J. R. Cheeseman, G. Scalmani, V. Barone, B. Mennucci, G. A. Petersson, H. Nakatsuji, M. Caricato, X. Li, H. P. Hratchian, A. F. Izmaylov, J. Bloino, G. Zheng, J. L. Sonnenberg, M. Hada, M. Ehara, K. Toyota, R. Fukuda, J. Hasegawa, M. Ishida, T. Nakajima, Y. Honda, O. Kitao, H. Nakai, T. Vreven, J. A. Montgomery, Jr., J. E. Peralta, F. Ogliaro, M. Bearpark, J. J. Heyd, E. Brothers, K. N. Kudin, V. N. Staroverov, T. Keith, R. Kobayashi, J. Normand, K. Raghavachari, A. Rendell, J. C. Burant, S. S. Iyengar, J. Tomasi, M. Cossi, N. Rega, J. M. Millam, M. Klene, J. E. Knox, J. B. Cross, V. Bakken, C. Adamo, J. Jaramillo, R. Gomperts, R. E. Stratmann, O. Yazyev, A. J. Austin, R. Cammi, C. Pomelli, J. W. Ochterski, R. L. Martin, K. Morokuma, V. G. Zakrzewski, G. A. Voth, P. Salvador, J. J. Dannenberg, S. Dapprich, A. D. Daniels, O. Farkas, J. B. Foresman, J. V. Ortiz, J. Cioslowski, and D. J. Fox, Gaussian, Inc., Wallingford CT, **2013**.

11. Lee, C. T.; Yang, W. T.; Parr, R. G. *Phys. Rev. B* **1988**, *37*,785-89.

12. Andersson, M. P.; Uvdal, P. *J. Phys. Chem. A* **2005**, 109, 2937-2941.

13. Kim, S.; Saracini, C.; Siegler, M. A.; Drichko, N.; Karlin, K. D. *Inorg. Chem.* **2012**, *51*, 12603-12605.